Journal of Geochemical Exploration 196 (2019) 33–41

Contents lists available at ScienceDirect

Journal of Geochemical Exploration

journal homepage: www.elsevier.com/locate/gexplo

A multidisciplinary investigation on bio-oxidation gold mine tailings from Dandong, China as a potential arsenic pollution source

Guoxin Huang[a,b], Ximing Luo[b,c,*], Daming Li[d], Zhitao Li[a], Zhaoxin Chen[c], Ming Zhu[e]

[a] Chinese Academy for Environmental Planning, Beijing 100012, China
[b] School of Ocean Sciences, China University of Geosciences (Beijing), Beijing 100083, China
[c] Beijing Key Laboratory of Water Resources & Environmental Engineering, China University of Geosciences (Beijing), Beijing 100083, China
[d] Shenzhen Institute of Building Research Co., Ltd., Shenzhen 518049, China
[e] China Meat Research Center, Beijing Academy of Food Sciences, Beijing 100068, China

ARTICLE INFO

Keywords:
Arsenic
Pollution source
Bio-oxidation tailings
Multi-characterisation
Fraction distribution
Release behavior

ABSTRACT

Very little is known about bio-oxidation tailings as an arsenic (As) pollution source. A comparison study was carried out between three flotation tailings (N1-1, N1-2 and N1-3) and three bio-oxidation tailings (N2-1, N2-2 and N2-3), collected from the Yangshu gold mine in China. A combined approach of mineralogy, geochemistry and environmental geochemistry was applied to explore geochemical and mineralogical properties, As fractions and its release behavior of the bio-oxidation tailings. The results showed that extremely high total As (TAs) of 25,200–27,100 μg/g (air-dry weight) observed in N2-1, N2-2 and N2-3 was about 30 times higher than that (616–940 μg/g) in N1-1, N1-2 and N1-3. The main elements were As, Ca, Fe and S, the mineral phases were gypsum ($CaSO_4$) (accounting for > 95 wt%), and the corresponding As was present as FeAsS and As_2O_5 in N2-1, N2-2 and N2-3. A larger amount of As in the water-soluble (5.80–9.98 μg/g), exchangeable (9.42–15.70 μg/g), carbonate-bound (29.23–63.36 μg/g) and Fe/Mn oxide-bound (5825–12,218 μg/g) fractions was found in N2-1, N2-2 and N2-3. Solution TAs released from N2-2 was higher than the level released from N1-1, and predominantly present in the oxidised form as arsenate As(V) in 192 h. The bio-oxidation tailings are able to release more As, and are a potential As pollution source of soil, surface and ground water.

1. Introduction

With the depletion of high-grade gold deposits, the minerals industry faces a significant challenge in the efficient processing of low-grade deposits with complex mineralogy (Tabatabaei et al., 2014). Low-grade refractory gold ores often contain finely, highly disseminated gold particles, and these gold particles are locked or wrapped within sulphide minerals such as pyrite, arsenopyrite, chalcopyrite and bornite (Feng and van Deventer, 2010; Kaksonen et al., 2014; Soltani et al., 2014). Although about 80% of the world's gold is pre-concentrated using flotation, numerous studies conducted in laboratories globally have indicated its low recovery for gold owing to ineffective destruction of a sulphide mineral (Williams et al., 2013; Tabatabaei et al., 2014).

In order to achieve a satisfactory gold recovery from low-grade refractory gold ores, other pre-treatment techniques have to be employed to destroy sulphide matrices, thereby exposing and liberating gold amenable to dissolution by chemical lixiviants (e.g., cyanidation). Among them, biological oxidation, as an alternative to conventional roasting and pressure oxidation, is receiving increased attention as a result of low production cost, low pressures, low temperatures, partial sulphide oxidation, decreased lixiviant consumption and no atmospheric pollution (Table 1) (La Brooy et al., 1994; Kaksonen et al., 2014). The bio-oxidation processes (BIOX, BioCOP, etc.) depend on the activity of acidophilic, chemolithotrophic, mesophilic (or thermophilic), Fe- and S-oxidising bacteria (or archaea) such as *Acidithiobacillus*, *Sulfobacillus*, *Ferroplasma*, *Acidithiobacillus caldus*, *Acidimicrobium ferrooxidans*, *Sulfobacillus thermosulfidooxidans* (Clark et al., 2006). The microorganisms mentioned above obtain energy by oxidising Fe^{2+} to Fe^{3+} or S^0 or other reduced S compounds to H_2SO_4 under strongly acidic, inorganic carbon-sufficient and dissolved oxygen-rich conditions. Apart from a direct enzymatic attack involving microorganism attachment to the mineral surfaces, indirect chemical oxidation by the resultant Fe^{3+} involving attacking the valence bonds gives rise to the destruction of sulphide matrices, as illustrated below for pyrite and arsenophyrite as examples (Eqs. (1)–(5)) (La Brooy et al., 1994; Clark et al., 2006; Huang and Li, 2014; Kaksonen et al., 2014).

---

[*] Corresponding author at: 29 Xueyuan Road, Haidian District, Beijing 100083, China.
E-mail address: xluocugb@126.com (X. Luo).

https://doi.org/10.1016/j.gexplo.2018.10.003
Received 6 September 2016; Received in revised form 3 August 2018; Accepted 4 October 2018

Table 1

Comparisons of economics and operating parameters among different pre-treatment techniques for low-grade refractory gold ores (La Brooy et al., 1994; Batty and Rorke, 2006; Brierley, 2008; Kaksonen et al., 2014).

Pretreament	Capital cost (US$ mill)	operating cost (US$/ton)	Total pressure (kPa)	Optimum temperature (°C)	Optimum pH
Roasting	4.9	56	/	650–700	/
Pressure oxidation	7.5	43	1100–3200[a]; 3300[b]	170-225[a]; 220[b]	/
Bio-oxidation	3.8	43	/	± 40[c] ± 78[d]	1.2–1.8[c] 1.5[d]

[a] Acid pressure oxidation.

[b] Alkaline pressure oxidation.

[c] BIOX®.

[d] BioCOP™.

These bio-processes have been developed successfully as an industrial application and applied commercially in China, Australia, America, Russia, South Africa, Brazil, Ghana, Peru, Ugana, Kazakstan and Uzbekistan since 1986 (Ndlovu, 2008; Kaksonen et al., 2014).

$$FeAsS[Au] + 3.5O_2 + 2.5H_2O \rightarrow 0.5Fe_2O_3 + SO_4^{2-} + 2H^+ + H_3AsO_4 + [Au] \quad (1)$$

$$FeS_2[Au] + 3.5O_2 + H_2O \rightarrow Fe^{2+} + 2SO_4^{2-} + 2H^+ + [Au] \quad (2)$$

$$Fe^{2+} + 0.25O_2 + H^+ \rightarrow Fe^{3+} + 0.5H_2O \quad (3)$$

$$FeS_2[Au] + 2Fe^{3+} \rightarrow 3Fe^{2+} + 2S^0 + [Au] \quad (4)$$

$$FeS_2[Au] + 14Fe^{3+} + 8H_2O \rightarrow 15Fe^{2+} + 2SO_4^{2-} + 16H^+ + [Au] \quad (5)$$

Gold mine tailings generated at mining, milling and smelting operations have become an important anthropogenic source of arsenic (As) contamination in soil, surface and ground water, and created considerable environmental and public health issues worldwide (Paktunc et al., 2004; de Mello et al., 2007; Grosbois et al., 2009; Toujaguez et al., 2013; Palapa and Maramis, 2015; Ko et al., 2012; Luo et al., 2016). Until now, the World Health Organization, the European Commission, and the US Environmental Protection Agency have all set up the maximum accepted level of As (10 μg/L) for drinking water regulations (Luo et al., 2016).

Prior to choosing a tailings disposal & management strategy and optimizing an environmental remediation design, it is very important and necessary to understand geochemical and mineralogical properties of tailings, determine distribution and speciation of As in tailings, and investigate mobility and stability of As in tailings. Accordingly, regarding different types of tailings, many researchers have particularly paid attention to the above aspects over the past decades. Paktunc et al. (2004) found that As- and Fe-bearing minerals were composed of iron (III) oxyhydroxides, scorodite, ferric arsenates, arseniosiderite, Ca-Fe arsenates, pharmacosiderite, jarosite and arsenopytite, and As occurred exclusively as As(V) resulting from cyanidation and SO_2/air processes in a cyanidation tailing from the Ketza River mine (Canada). Hamberg et al. (2016) observed that the aqueous As ranged from 22 to 554 μg/L, and most of the As (94.6 wt%) was associated with the secondary Fe(III) minerals in another cyanidation tailing from the Svartliden gold mine (Sweden). Schippers et al. (2008) noted that As- and Fe-bearing minerals were comprised of galena, sphalerite, pyrite, arsenopyrite, stibnite and chalcopyrite in a flotation tailing from the Ticapampa tailings dump (Peru). Martínez et al. (2016) showed that the mean As level was 180 μg/g and the pH value ranged from 6.7 to 8.2 in another flotation tailing from the Linares-La Carolina mining district (Spain). Toujaguez et al. (2013) pointed out that As- and Fe-bearing minerals consisted of arsenopyrite, Fe-arsenates and goethite, scorodite-oxidation state As(V) was dominant, and the mean As content was 35,372 μg/g in a calcination tailing from the Delita gold mining area (Cuba). Clearly, bio-oxidation tailings have been neglected for a long time in previous studies. In other words, data on their geochemistry and minerology are rather scarce, and information on As fractionation, speciation and release is pretty inadequate.

Here, we report a comparison study carried out between samples from three flotation tailings and three bio-oxidation tailings from the Yangshu gold mine, China. The objectives of this study were to: (1) characterise the bio-oxidation tailings using various geochemical and mineralogical analyses; (2) determine the As distribution in the six geochemical fractions of them using a sequential chemical extraction procedure; (3) investigate the As release behavior from them under different pH values using batch leaching tests; and (4) identify their potential occurrence of arsenic pollution from them.

2. Materials and methods

2.1. Description of tailings samples and sites

Three solid flotation tailings samples (named N1-1, N1-2 and N1-3) (grey; 20 cm in depth) were collected from the first historic gold mine tailings dump (40°43′12″N 123°41′24″E), which have been deposited for 1, 90 and 365 days before sampling, respectively (Fig. 1a, b, d). Simultaneously, three solid bio-oxidation tailings samples (named N2-1, N2-2 and N2-3) (red brown; 20 cm in depth) were drawn from the second tailings dump (40°40′12″N 123°58′48″E), which have been aged for 1, 90 and 365 days, respectively (Fig. 1a, c, e). The tailings sampling was repeated four times at depths of 45–55 cm in an area of 1 m^2 around a sampling point to obtain four subsamples (each 2 kg). Subsequently, a composit, homogenous, representative sample (8 kg) was taken by mixing them well at each sampling point, and then directly placed in a pre-cleaned, opaque, air-free polyethylene sealable bag. Following collection, the six samples were stored and shipped in a cooler box with ice. On return to the laboratory, all the samples were gently air-dried at room temperature (20 ± 2 °C), rolled to break up macro-aggregates and finally passed through a 200 mesh stainless steel sieve to remove coarse debris. After a manual homogenization, the samples were stored in the dark before use.

Both tailings dumps, belonging to the Yangshu gold mine in the east of the Qingchengzi ore field, are located in Fengcheng, Dandong, Liaoning, China, and are one or more kilometers in diameter in the environments. The region of Fengcheng is subjected to a typical continental monsoon climate, warm and wet in summer, cold and relatively dry in winter. The maximum/minimum annual average temperature is 36.5/−33.8 °C with strong seasonal temperature variations. The rainfall is strong and seasonal with a maximum/minimum annual average value of 1386/873 mm (mostly in June, July, August and September). In addition, the annual average evaporation rate and frostless season are 860 mm and 156 days, respectively.

2.2. Reagents and reference materials

Standard reference materials GBW08605, GBW08611, GBW08666 and GBW08667 for analysis of total As (TAs), As(III) and As(V) and

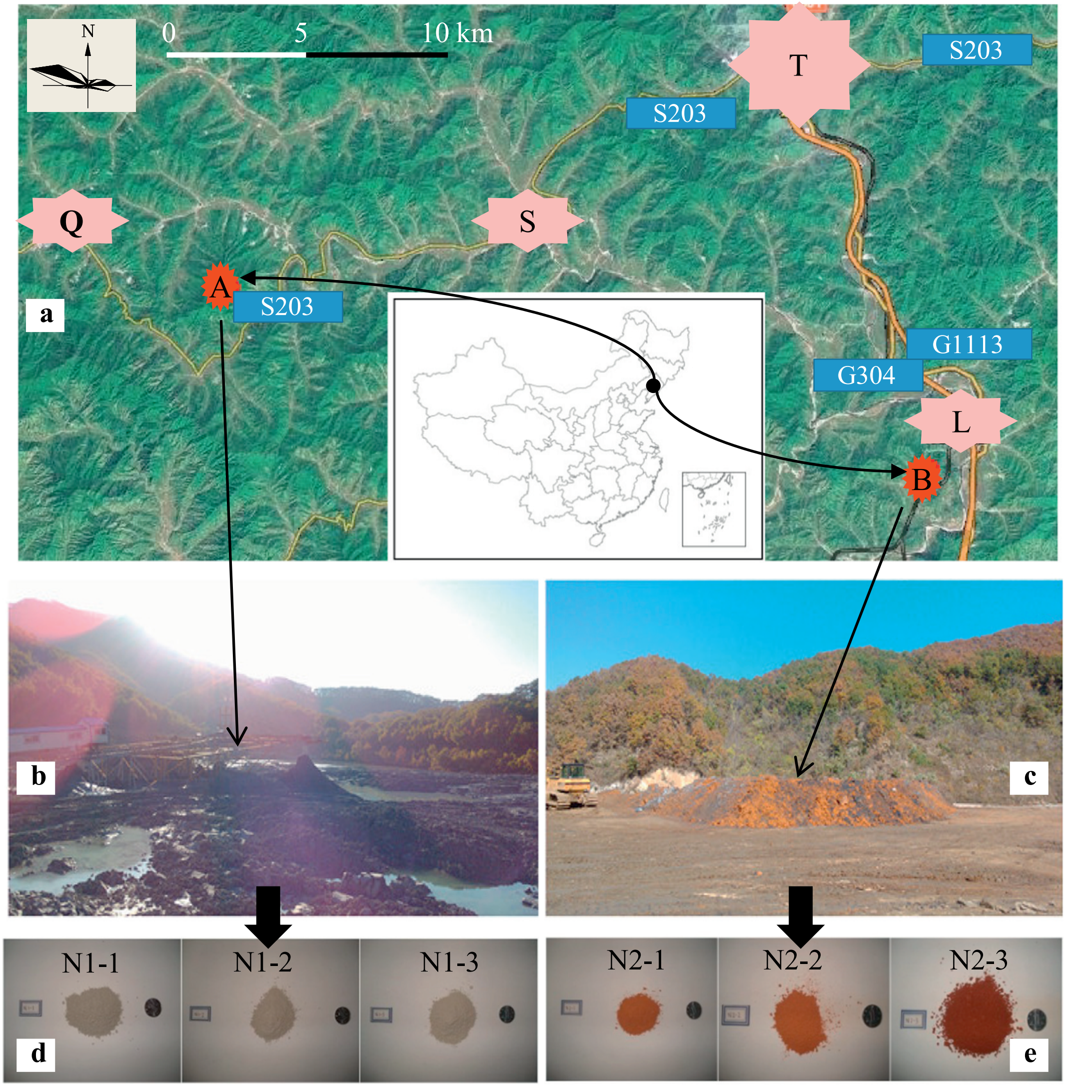

Fig. 1. Locations of the tailings sampling sites (a). N indicates north. A represents the flotation tailings dump (40°43′12″N 123°41′24′E). B represents the bio-oxidation tailings dump (40°40′12″N 12358′48″E). Q, S, T and L respectively represent Qingchengzi Town, Simenzi Town, Tongyuanpu Town and Liujiahe town. S203, G304 and G1113 respectively represent Dandong-Dalian provincial road, Dandong-Huolinguole national road and Dandong-Fuxin highway road. Photograph of the flotation tailings dump (b). Photograph of the bio-oxidation tailings dump (c). Photograph of the flotation tailings samples in the laboratory, showing N1-1, N1-2 and N1-3 whose deposition periods are respectively 1, 90 and 365 days (d). Photograph of the bio-oxidation tailings samples in the laboratory, showing N2-1, N2-2 and N2-3 whose deposition periods are respectively 1, 90 and 365 days (e). (For interpretation of the references to color in this figure legend, the reader is referred to the web version of this article.)

certified reference material GBW07444 (GSF-4) for As sequential extractions were obtained from National Institute of Metrology, Beijing, China. All reagents used were trace metal, analytical grade or better as received, and all solutions were prepared using ultrapure water with a minimum resistance of 18.2 MΩ·cm (Milli-Q, Millipore Corp., Billerica, MA, USA).

2.3. Geochemical and mineralogical characterisation of gold mine tailings

The flotation (N1-1, N1-2, N1-3) and bio-oxidation (N2-1, N2-2, N2-3) tailings samples were characterised by analysing geochemical properties and mineralogical compositions. Paste pH was measured at a solid: liquid ratio of 1: 2.5 after a contact period of 48 h using a digital pH meter (Sartorius, PB-10, Germany). TAs was determined in the same tailings slurry using an inductively coupled plasma atomic emission spectrometer (ICP-AES) with a lower detection limit of 0.15 mg/L (Thermo, IRIS Advantage, USA) and an inductively coupled plasma mass spectrometer (ICP-MS) with a lower detection limit of 0.12 μg/L (Thermo, X-series, USA) after acid digestion (HF + HCl + $HClO_4$ + HNO_3). pH point of zero charge (pH_{PZC}) was estimated using batch equilibrium techniques (adsorbent amount 0.2 g, background electrolyte 40 mL 0.1 M KNO_3, contact temperature 20 ± 1 °C, reaction time 24 h), following the procedure proposed by Chutia et al. (2009). Oxidation-reduction potential (ORP) was monitored on-site immediately after tailings sampling using an ORP depolarization automatic analyzer (Nanjing Chuan-Di Instrument & Equipment Co., Ltd., FJA-6, China). In each chemical analysis, at least one in five samples was duplicated and the deviation between the two samples was always $< 5\%$. Morphology and chemical composition were simultaneously identified using scanning electron microscopy (SEM) (20 kV) (ZEISS, EVO18, Germany) coupled with energy dispersive spectroscopy (EDS) (20 kV) (Bruker, XFlash Detector 5010, Germany). Chemical composition was also identified using wavelength-dispersive X-ray fluorescence (WDXRF) spectrometry equipped with 4 kW power and a Rh tube for the generation of X-rays (PANalytical, AXIOS, the Netherland). Crystal phases were determined using semi-quantitative X-ray diffraction (XRD)

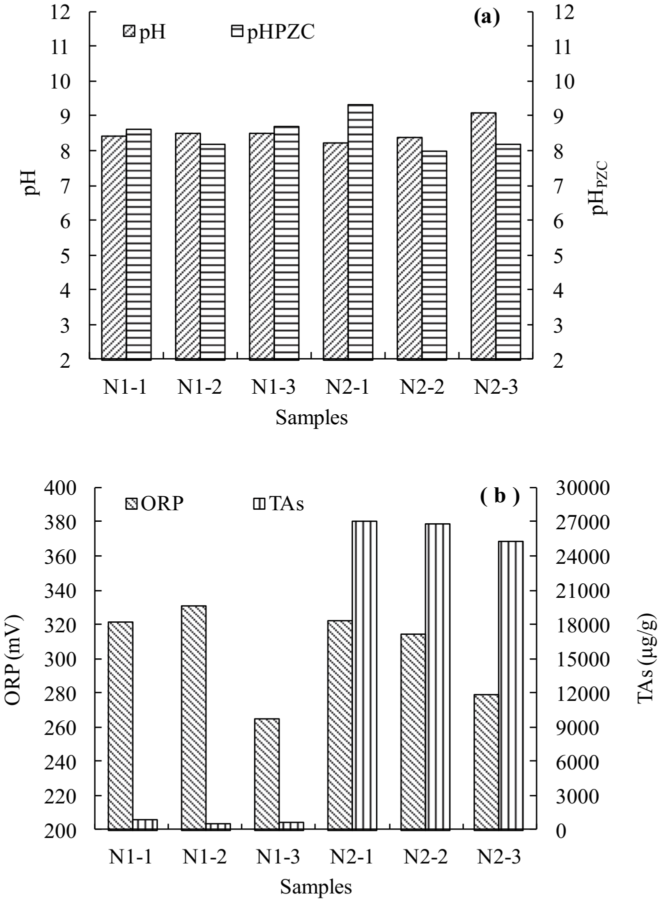

Fig. 2. Geochemical properties of gold mine tailings samples: pH and pH point of zero charge (pH_{pzc}) (a); oxidation-reduction potential (ORP) and total arsenic (TAs) (b) (solid: liquid ratio 1: 2.5, contact time 48 h).

spectrometry equipped with a rotating anode and Cu-Kα radiation (40 kV, 100 mA, 6° 2θ/min, 2.6–45°) (Rigaku, D/max 2500, Japan), and their relative proportions were calculated from the peak heights of the XRD spectra. Arsenic and iron species were investigated using electron probe micro-analysis (EPMA) (15 or 20 kV, 10 nA, counting time 20 s) (JEOL, JXA-8230, Japan). Pyrite and scorodite were used as analytical and calibration standards (DeSisto et al., 2011).

2.4. Chemical fractionation of arsenic in gold mine tailings

Arsenic distribution in the different fractions of the six tailings samples (N1-1, N1-2, N1-3, N2-1, N2-2 and N2-3) was determined by a sequential chemical extraction procedure. Considering the alkaline pHs of the tailings used (Fig. 2a), the sequential chemical extraction procedure modified from Tessier et al. (1979), Wan et al. (2006), Rodríguez-Vila et al. (2015) and Bisone et al. (2016) was performed to extract six As fractions. Water-soluble fraction (F1): a tailings sample (0.50 g) (or a certified reference material GBW07444 (1.00 g)) was extracted with 10 mL ultrapure water for 2 h on a shaker at 25 ± 2 °C. Exchangeable fraction (F2): the residue from F1 was extracted with 10 mL 1 M $MgCl_2$ at pH 7.0 for 2 h on a shaker at 25 ± 2 °C. Carbonate-bound fraction (F3): the residue from F2 was extracted with 10 mL 1 M CH_3COONa at pH 5.0 (adjusted with CH_3COOH) for 5 h on a shaker at 25 ± 2 °C. Fe/Mn oxide-bound fraction (F4): the residue from F3 was extracted with 20 mL 0.25 M $NH_2OH{\cdot}HCl$ in 0.25 M HCl at pH 3.0 (adjusted with HCl) for 6 h on a shaker at 25 ± 2 °C. Organic matter-bound fraction (F5): the residue from F4 was extracted with 3 mL 0.02 M HNO_3 and 5 mL 30% H_2O_2 at pH 2.0 (adjusted with HNO_3) for 1.5 h in a water bath at 83 ± 3 °C with occasional agitation. Another aliquot of 3 mL 30% H_2O_2 was added and heated again at pH 2.0 (adjusted with HNO_3) for 1.2 h at 83 ± 3 °C with intermittent agitation. After cooling to room temperature, 2.5 mL 3.2 M CH_3COONH_4 in 3.2 M HNO_3 was added. The sample was diluted to 25 mL with ultrapure water, agitated continuously for 40 min and finally kept standing for 10 h. And residual fraction (F6): the residue from F5 (0.10 g, dry weight) was extracted with 20 mL aqua regia (HNO_3: HCl = 1: 3) for 3 h in a water bath at 90 ± 3 °C. Following each extraction, the mixtures were centrifuged at 3000 rpm for 15 min. The solid pellets were washed with 10 mL ultrapure water and centrifuged twice. The amount of As recovered in the washing step was added to the next step before the washing (Rodríguez-Vila et al., 2015). The supernatants were filtered through 0.45-μm acetate-cellulose filter membranes. The resultant filtrates were preserved via adding 1–2 drops of 10% HNO_3 solution and then stored at 4 °C until analysis. Each extraction step was performed in triplicate. TAs was determined by ICP-AES and ICP-MS (see Section 2.3.). The relative standard deviation of the sequential chemical extraction procedure was $<$ 8%, and its recovery varied in the range of 87% and 110%.

2.5. Arsenic leaching tests

Arsenic release behavior in the flotation (N1-1) and bio-oxidation (N2-2) tailings samples was investigated under different environmental conditions. A series of batch leaching tests were carried out in triplicates in 56 50-mL screw-capped plastic centrifuge tubes at a solid: liquid ratio of 1: 10 (Coussy et al., 2011; Kim et al., 2016). To investigate As release under different pH conditions considering the occasional occurrence of acid rain, 15 mL 0.1 M NaOH and 1.5 g (air-dry weight) N1-1 was added into centrifuge tubes 1–21, and 15 mL 0.1 M NaOH and 1.5 g (air-dry weight) N2-2 into centrifuge tubes 22–42. The initial solution pH was adjusted with 0.1 M NaOH and 0.1 M HCl, yielding pHs of 5.00, 8.04, 9.10, 5.00, 8.04 and 8.73 in centrifuge tubes 1–7, 8–14, 15–21, 22–28, 29–35 and 36–42, respectively. To investigate As release in the presence of phosphate considering its probable promoting effect in As mobility (Grosbois et al., 2011), 15 mL 0.32 M NaH_2PO_4 and 1.5 g (air-dry weight) N1-1 was added into centrifuge tubes 43–49, and 15 mL 0.32 M NaH_2PO_4 and 1.5 g (air-dry weight) N2-2 into centrifuge tubes 50–56. All the substances in each centrifuge tube were mixed well manually at the beginning of the tests and kept standing at room temperature for different preset time intervals (1, 4, 16, 48, 96, 144 and 192 h). The resultant mixtures were centrifuged at 3000 rpm for 15 min. The supernatants were filtered through 0.45-μm glass-fiber filter membranes. The filtrates were placed in 15-mL screw-capped plastic tubes, and finally stored with acidification (10% HNO_3, pH $<$ 2) at 4 °C in an effort to avoid a change in As speciation prior to analysis for pH, TAs, As(III) and As(V). pH was measured with a digital pH meter before acidification (see Section 2.3.). TAs was determined with ICP-AES and ICP-MS (see Section 2.3.). As(V) and As(III) were determined with a high-performance liquid chromatograph (HPLC) (Agilent, 1100 Series, USA) composed of a system controller, a solvent delivery module, a column oven and a 6-port injection valve and equipped with a reversed-phase C18 column (Capcell, Pak, 250 mm × 4.6 mm, 5 μm particle size) for separation of As species in combination of ICP-MS acting as a detector (Agilent, 7500C, USA).

3. Results and discussion

3.1. Characterisation of bio-oxidation tailings

3.1.1. Geochemical properties

Fig. 2 presents the geochemical properties of samples N1-1, N1-2, N1-3, N2-1, N2-2 and N2-3. pH of 8.23 for N2-1 was lower than the pH_{pzc} of 9.3 (Fig. 2a), resulting in a net positive surface charge; meanwhile pHs of 8.37 for N2-2 and 9.08 for N2-3 were higher than the corresponding pH_{pzc}s of 8.0 and 8.2, respectively (Fig. 2a), resulting in a net negative surface charge (Manasse and Viti, 2007). ORP dropped as deposition time increased to 365 days (Fig. 2b). These observations indicated that (1) bio-oxidation tailings were invariably alkaline over time, (2) their surface charge properties were changeable over time, and (3) their redox potentials were unstable over time. These behaviors will not only influence As species and mobility (Garelick et al., 2005; Bisone et al., 2016), but also make many remediation technologies inefficient (Baek et al., 2009; Wang et al., 2014). Surprisingly, extremely high TAs in the range of 25,200–27,100 μg/g (air-dry weight) was observed in N2-1, N2-2 and N2-3, which was about 30 times higher than that (616–940 μg/g) (air-dry weight) in N1-1, N1-2 and N1-3 (Fig. 2b) and 46.3 times higher than that (544 μg/g) in the abandoned La Aquisgrana mine tailings (Martínez et al., 2016). It is evident that a bio-oxidation process but not a flotation process is able to release more As. This was attributed to more breakdown of the crystal lattice structure of arsenopyrite in the presence of microorganisms (Eq. (1)) (Soltani et al., 2014). Actually, flotation does not destroy the matrices of arsenopyrite, as flotation depending on collector electrochemical sorption to form hydrophobic coatings on Au- and Fe-bearing species is a physicochemical process (Allan and Woodcock, 2001; Dunne, 2005; Yalcin and Kelebek, 2011). Undoubtedly, the alkaline nature, the decreased redox potential, the changeable surface charges property and the high TAs demonstrated that the bio-oxidation tailings were a potential As pollution source.

3.1.2. *Morphological characteristics*

Fig. 3 presents the morphology of samples N1-1, N1-2, N1-3, N2-1, N2-2 and N2-3, which was determined by SEM microscopy. For the two tailings types, nearly all the particles were smaller than 70 μm in diameter and had no pits (Fig. 3a to f). Furthermore, these particles were separated from each other (i.e., they were not aggregated), around which there existed a lot of voids (Fig. 3a to f). In comparison to N1-1, N1-2 and N1-3, N2-1, N2-2 and N2-3 tended to show a higher number of regular, small and granular grains (Fig. 3a to f). Also, the bio-oxidation tailings seemed to show more pits visible on the surfaces of some grains (Fig. 3e, f). Biochemical breakdown of sulphide minerals leads to producing pitting and etching of their surfaces and even complete dissolution of mineral grains (Kaksonen et al., 2014).

3.1.3. *Elemental compositions*

Table 2 and Fig. 4 present the chemical compositions of samples N1-1, N1-2, N1-3, N2-1, N2-2 and N2-3, which were determined by WDXRF spectrometry and EDS spectroscopy, respectively. There was a big difference in elemental content between the two tailings types: the contents of Si, Al, Mg and K in N1-1, N1-2 and N1-3 were greater than those in N2-1, N2-2 and N2-3; in contrast, the contents of Ca, Fe and S in N2-1, N2-2 and N2-3 were much larger than those in N1-1, N1-2 and N1-3 (Table 2). These results implied the difference in crystalline minerals between the two tailings types. It should be noted that no As was detected by WDXRF (Table 2) likely due to its content being below detection limit, but the EDS spectra indicated its presence in all the tailings (Fig. 4a to f). More importantly, at the deposition time of 365 days, a larger amount of As was observed in N2-3 (25.66 wt%) compared to N1-3 (14.37 wt%) (Fig. 4c, f). This also demonstrated that the bio-oxidation tailings were a potential As pollution source.

3.1.4. *Crystalline minerals*

Fig. 5 presents the crystalline mineral phases of samples N1-1, N1-2, N1-3, N2-1, N2-2 and N2-3, which were determined by XRD spectrometry. The flotation tailings (N1-1, N1-2 and N1-3) were mainly comprised of quartz (SiO_2), dolomite ($CaMg(CO_3)_2$) and clay-type minerals (accounting for > 87 wt%), whereas the bio-oxidation tailings (N2-1, N2-2 and N2-3) were dominantly composed of gypsum ($CaSO_4$) (accounting for > 95 wt%) (Fig. 5). Apparently, these mineral phases were roughly in accordance with the chemical components, as illustrated by the EDS and WDXRF data (Fig. 4a to f and Table 2). On the other hand, unlike the flotation tailings, the dominant crystalline mineral (gypsum) in the bio-oxidation tailings was maintained nearly invariably with increasing deposition time (Fig. 5). In bio-oxidation processes, sulphuric acid as a pH regulator is added into the reactors to control the extremely low pHs (Table 1), and meanwhile limestone as a carbon source is added to ensure the metabolism of acidophilic,

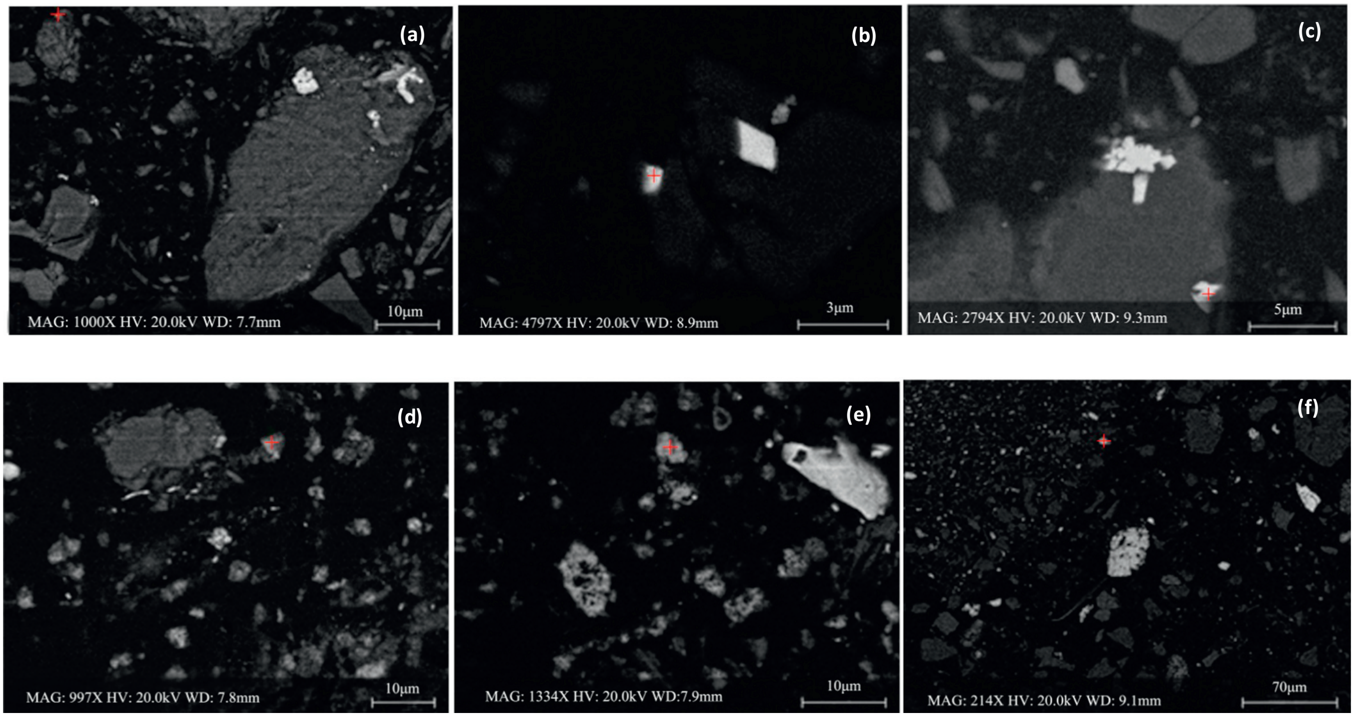

Fig. 3. Micro-structures of gold mine tailings samples (N1-1 (a); N1-2 (b); N1-3 (c); N2-1 (d); N2-2 (e); N2-3 (f)) determined by scanning electron microscopy (20 kV).

Table 2

Chemical components of gold mine tailings samples (N1-1, N1-2, N1-3, N2-1, N2-2 and N2-3) determined by wavelength-dispersive X-ray fluorescence spectrometry equipped with 4 kW power and a Rh tube.

Samples	Si (wt%)	Al (wt%)	Ca (wt%)	Mg (wt%)	K (wt%)	Fe (wt%)	Mn (wt%)	S (wt%)	Others (wt%)
N1-1	56.9	13.1	6.3	4.3	4.7	3.1	0.1	0.7	10.8
N1-2	56.6	10.3	7.8	5.5	3.6	2.7	0.1	0.5	12.9
N1-3	57.6	8.8	8.3	5.6	3.2	2.3	0.1	0.5	13.6
N2-1	5.5	1.8	22.0	1.9	0.3	17.3	0.1	22.7	28.4
N2-2	4.0	1.3	21.1	1.7	0.2	19.4	0.1	23.4	28.8
N2-3	4.7	1.6	22.4	1.8	0.3	17.3	0.1	23.9	27.9

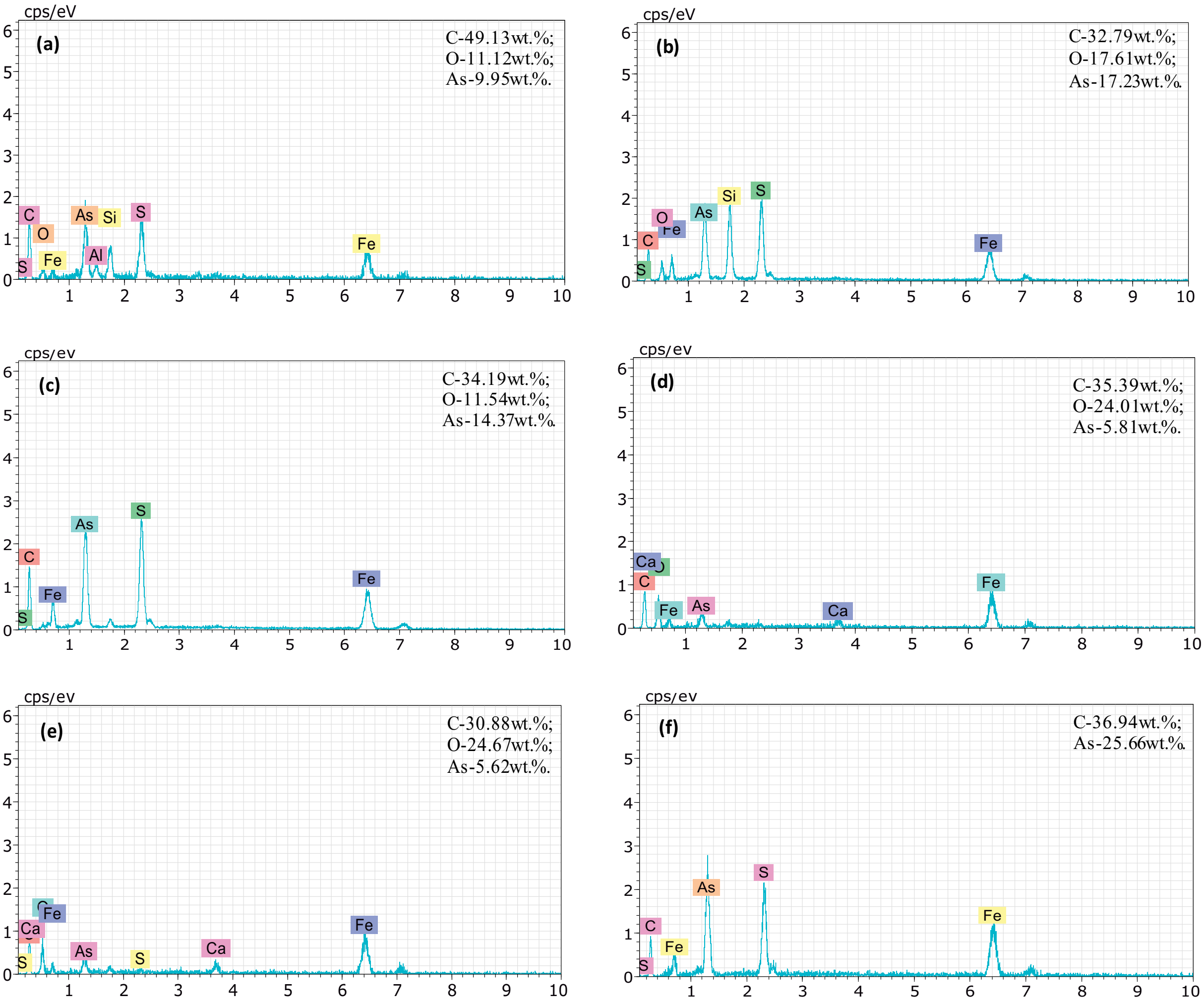

Fig. 4. Elemental compositions of gold mine tailings samples (N1-1 (a); N1-2 (b); N1-3 (c); N2-1 (d); N2-2 (e); N2-3 (f)) determined by energy dispersive spectroscopy (20 kV).

chemolithotrophic microorganisms (Kaksonen et al., 2014). Furthermore, alkaline substances (e.g., lime) must be added into bio-oxidised concentrates and process effluents in order to neutralise acid and create an alkaline condition for extracting gold with cyanide or thiosulphate and precipitating metal(loid)s (Ritcey, 2005; Feng and van Deventer, 2010; Kaksonen et al., 2014; Soltani et al., 2014). For these reasons, large amounts of Ca^{2+} and SO_4^{2-} are introduced into the bio-oxidation systems, and eventually a dominant amount of secondary gypsum is formed in the bio-oxidation tailings (Fig. 5).

Even though high proportions of As and Fe elements were determined (Fig. 4d to f and Table 2), no corresponding crystallised As- and Fe-bearing minerals were detected in the bio-oxidation tailings by XRD (Fig. 5). Fortunately, the EPMA analysis showed that As and Fe were present as FeS_2, FeAsS and As_2O_5 in the bio-oxidation tailings. In practice, only partial oxidation of sulphides is required because in most cases gold is concentrated at the grain boundaries and other preferred sites (La Brooy et al., 1994). As_2O_5 was present in Fe(III) arsenate (Parviainen et al., 2012) generated via FeAsS and FeS_2 bio-oxidation as a secondary mineral (Eqs. (1)–(3)). A previous study found that As and Fe were present as iron (III) oxyhydroxides, $FeAsO_4{\cdot}2H_2O$, ferric arsenates, $Ca_2Fe_3(AsO_4)_3O_2{\cdot}3H_2O$, Ca-Fe

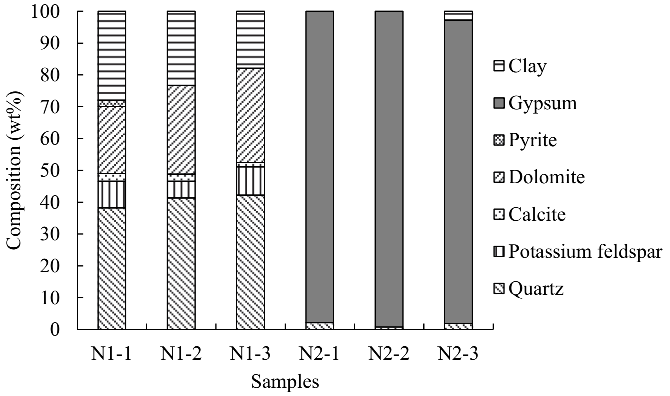

Fig. 5. Crystalline minerals of gold mine tailings samples determined by X-ray diffraction spectrometry (40 kV, 100 mA, 6° 2θ/min, 2.6–45°).

Table 3
Arsenic distribution in the different fractions of gold mine tailings. Arsenic fractions are F1 (water-soluble), F2 (exchangeable), F3 (carbonate-bound), F4 (Fe/Mn oxide-bound), F5 (organic matter-bound) and F6 (residual). Data points represent the average of triplicate samples.

Sample		N1-1	N1-2	N1-3	N2-1	N2-2	N2-3
F1	(μg/g)	1.50	1.55	3.22	5.80	9.87	9.98
	(wt%)	0.14	0.23	0.39	0.01	0.01	0.01
F2	(μg/g)	1.61	2.04	3.27	9.42	13.44	15.70
	(wt%)	0.15	0.30	0.40	0.01	0.02	0.02
F3	(μg/g)	2.96	3.35	5.34	29.23	33.25	63.36
	(wt%)	0.28	0.50	0.65	0.03	0.04	0.09
F4	(μg/g)	76.64	47.95	73.57	10,278	12,218	5825
	(wt%)	7.12	7.09	8.91	11.05	16.34	7.90
F5	(μg/g)	51.58	50.83	74.64	170.6	359.6	178.0
	(wt%)	4.79	7.52	9.04	0.18	0.48	0.24
F6	(μg/g)	942.2	570.1	666.0	82,503	62,122	67,635
	(wt%)	87.53	84.36	80.63	88.72	83.10	91.74
MF	(wt%)	0.57	1.03	1.44	0.05	0.07	0.12

arsenates, $KFe_4(AsO_4)_3(OH)_4 \cdot 6–7H_2O$, $K_2Fe_6(SO_4)_4(OH)_{12}$ and FeAsS in cyanidation tailings (Paktunc et al., 2004). Apparently, different tailings types were composed of different As- and Fe-bearing minerals.

3.2. Arsenic distribution in the different fractions of bio-oxidation tailings

Table 3 presents the arsenic distribution in the different fractions of samples N1-1, N1-2, N1-3, N2-1, N2-2 and N2-3, which were extracted by the sequential chemical extraction procedure. The index of the mobility of As was calculated as a mobility factor (*MF*) according to Eq. (6) (Rodríguez-Vila et al., 2015).

$$MF = (F1 + F2 + F3)/(F1 + F2 + F3 + F4 + F5 + F6) \times 100 \qquad (6)$$

In N2-1, N2-2 and N2-3, As fractions from highest to lowest were F6 (83.10–91.74 wt%) ≫ F4 (7.90–16.34 wt%) ≫ F5 (0.18–0.48 wt%) > F3 (0.03–0.09 wt%) > F2 (0.01–0.02 wt%) > F1 (0.01 wt%) (Table 3). There is no doubt that the first and second dominant As fractions were the residual (F6) and Fe/Mn oxide-bound (F4) fractions, respectively. The residual As exists in a lattice of silicates and other primary and secondary minerals (Chen et al., 2016), indicating that it is not easily released over a reasonable time span under the conditions normally encountered in nature (Tessier et al., 1979). The Fe/Mn oxide-bound As is present in Fe and Mn oxides via adsorption and co-precipitation as nodules, concretions and cement between mineral particles or simply as coatings on mineral particles (Tessier et al., 1979). The F4 fraction fluctuated with deposition time (Table 3), confirming that the As in this fraction did not stay stable. Therefore, the As in the F4 fraction should be considered as a potential source of labile As. N2-1, N2-2 and N2-3 have been deposited for 1, 90 and 365 days, respectively, indicating that they are exposed to different climate conditions. This could be regarded as a cause of the F4 fraction fluctuation. Compared to the flotation tailings, despite the lower proportions of As in the F1 (≤ 0.02 wt%), F2 (≤ 0.01 wt%) and F3 (≤ 0.09 wt%) fractions

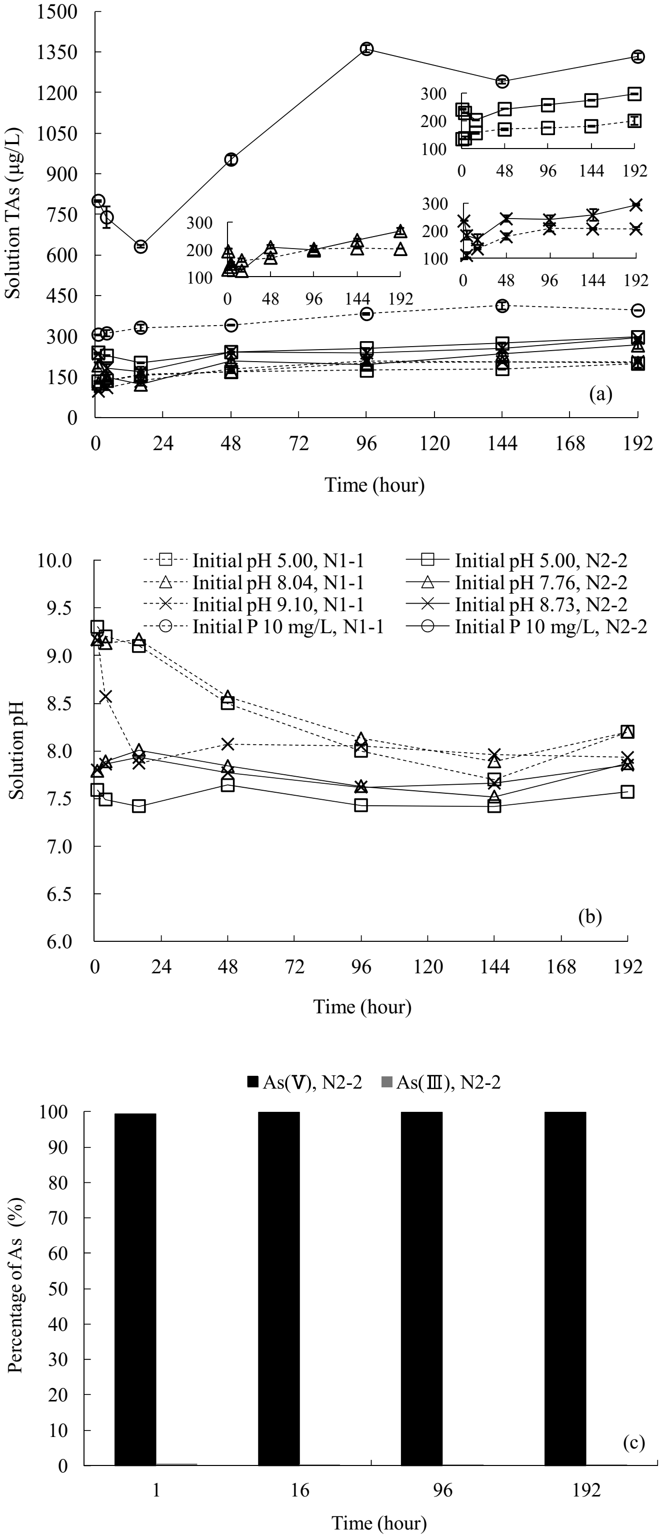

Fig. 6. As release behavior over time in the batch leaching tests: solution total arsenic (TAs) (a); solution pH (b); percentages of As(V) and As(III) present in the solution (c). Data points and error bars represent the average of triplicate samples and standard deviation, respectively. Experimental conditions and As species are given in the legend, together with sample names.

with a lower *MF*, the bio-oxidation tailings potentially posed a greater threat to environment, as evidenced by a larger amount of As content in the F1 (5.80–9.98 μg/g), F2 (9.42–15.70 μg/g), F3 (29.23–63.36 μg/g) and F4 (5825–12,218 μg/g) fractions (Table 3).

3.3. Arsenic release behavior in bio-oxidation tailings

Fig. 6 presents the changes in solution TAs and pH as well as As species over time in the batch leaching tests. TAs (between 122.3 ± 4.2 and 296.7 ± 12.2 μg/L) released from N2-2 was found to be higher than the level (between 97.7 ± 2.5 and 207.4 ± 12.4 μg/L) released from N1-1 in 192 h under the initial acidic and alkaline pHs (Fig. 6a). For N2-2, TAs increased linearly and remarkably with time increasing from 96 to 192 h at the initial pHs of 5.00, 7.76 and 8.73, respectively (Fig. 6a). TAs peaks of 296.7 ± 12.2, 266.7 ± 12.2 and 293.5 ± 19.8 μg/L appeared at 192 h at the three initial pHs, which corresponded to only 30.06 ± 1.24%, 27.02 ± 1.24% and 29.74 ± 2.01% of the soluble As fraction, respectively (Fig. 6a and Table 3). The above TAs change trends and percent values implied that more As might be released if time was further increased (> 192 h), considering the large amount of As in the solube (9.87 μg/g), exchangeable (13.44 μg/g), carbonate-bound (33.25 μg/g) and even Fe/Mn oxide-bound (12,218 μg/g) fractions (Table 3).

Unlike TAs, pH (7.42–8.01) for N2-2 was lower than that (7.70–9.30) for N1-1 after 1 h under the different initial pH conditions (Fig. 6b). The more steady pH suggested that bio-oxidation tailings had a higher capacity of quickly buffering pH. Under the conditions of pH (7.42–8.01) and ORP (300 ± 20 mV) tested here, aqueous As released from N2-2 was predominantly present in the oxidised form of arsenate As(V) as the negatively charged oxyanion $HAsO_4^{2-}$ (Tabelin et al., 2014), accounting for ≥99.47% of the solution TAs (Fig. 6b, c).

High TAs ranging from 631.5 ± 5.7 to 1362 ± 12 μg/L was observed at any time point in the presence of phosphate for N2-2, which was 4.1–6.9 times higher than that in the absence of phosphate (initial pH 7.76), and meanwhile 1.9–3.6 times higher than that in the presence of phosphate for N1-1 (Fig. 6a). These results indicated that phosphate promoted the As release in the bio-oxidation tailings. Phosphate competes strongly with As (especially arsenate) for available exchange sites on Fe and Mn oxides (Guo et al., 2008). The competing effect coupled with the more Fe/Mn oxide-bound As (Table 3) can be employed to explain the greater As release from bio-oxidation tailings in the presence of phosphate.

4. Conclusions

The bio-oxidation tailings were a potential As pollution source mainly due to biochemical breakdown of the crystal lattice structure of arsenopyrite and readily changeable environmental conditions over deposition time.

Based on their multi-characterisation, the bio-oxidation tailings had extremely high TAs with invariably alkaline pHs, changeable surface charges and unstable redox potentials. Simultaneously, their main elements (As, Ca, Fe and S), mineral phases (gypsum) and As minerals (mainly FeAsS and As_2O_5) were maintained nearly constant with increasing deposition time.

Based on their As distribution, even though As fractions were, in the descending order, F6 (83.10–91.74 wt%) ≫ F4 (7.90–16.34 wt%) ≫ F5 (0.18–0.48 wt%) > F3 (0.03–0.09 wt%) > F2 (0.01–0.02 wt%) > F1 (0.01 wt%), there was a large As content in the F1 (5.80–9.98 μg/g), F2 (9.42–15.70 μg/g), F3 (29.23–63.36 μg/g) and F4 (5825–12,218 μg/g) fractions, i.e., in easily mobilizable fractions.

Based on their As release behavior, the peaks of solution TAs released from N2-2 appeared at 192 h at the initial pHs of 5.00, 7.76 and 8.73, respectively. Aqueous As was predominantly present in the oxidised form as arsenate As(V). Phosphate promoted the As release in the bio-oxidation tailings, due to its competition with As (especially arsenate) for available exchange sites.

Acknowledgments

This study is financially supported jointly by NSFC (41172226) and the project from the China Geological Survey (DD20160312).

References

Allan, G.C., Woodcock, J.T., 2001. A review of the flotation of native gold and electrum. Miner. Eng. 14, 931–962.

Baek, K., Kim, D.-H., Park, S.-W., Ryu, B.-G., Bajargal, T., Yang, J.-S., 2009. Electrolyte conditioning-enhanced electrokinetic remediation of arsenic-contaminated mine tailing. J. Hazard. Mater. 161, 457–462.

Batty, J.D., Rorke, G.V., 2006. Development and commercial demonstration of the BioCOP™ thermophile process. Hydrometallurgy 83, 83–89.

Bisone, S., Chatain, V., Blanc, D., Gautier, M., Bayard, R., Sanchez, F., Gourdon, R., 2016. Geochemical characterization and modeling of arsenic behavior in a highly contaminated mining soil. Environ. Earth Sci. 75, 306.

Brierley, J.A., 2008. A perspective on developments in biohydrometallurgy. Hydrometallurgy 94, 2–7.

Chen, X., Ji, H., Yang, W., Zhu, B., Ding, H., 2016. Speciation and distribution of mercury in soils around goldmines located upstream of Miyun Reservoir, Beijing, China. J. Geochem. Explor. 163, 1–9.

Chutia, P., Kato, S., Kojima, T., Satokawa, S., 2009. Arsenic adsorption from aqueous solution on synthetic zeolites. J. Hazard. Mater. 162, 440–447.

Clark, M.E., Batty, J.D., van Buuren, C.B., Dew, D.W., Eamon, M.A., 2006. Biotechnology in minerals processing: technological breakthroughs creating value. Hydrometallurgy 83, 3–9.

Coussy, S., Benzaazoua, M., Blanc, D., Moszkowicz, P., Bussière, B., 2011. Arsenic stability in arsenopyrite-rich cemented paste backfills: a leaching test-based assessment. J. Hazard. Mater. 185 (2), 1467–1476.

DeSisto, S.L., Jamieson, H.E., Parsons, M.B., 2011. Influence of hardpan layers on arsenic mobility in historical gold mine tailings. Appl. Geochem. 26, 2004–2018.

Dunne, R., 2005. Flotation of gold and gold-bearing ores. In: Adams, M.D. (Ed.), Developments in Mineral Processing. vol. 15. Elsevier, Amsterdam, pp. 309–343.

Feng, D., van Deventer, J.S.J., 2010. Oxidative pre-treatment in thiosulphate leaching of sulphide gold ores. Int. J. Min. Sci. Technol. 94, 28–34.

Garelick, H., Dybowska, A., Valsami-Jones, E., Priest, N.D., 2005. Remediation technologies for arsenic contaminated drinking waters. J. Soils Sediments 5, 182–190.

Grosbois, C., Schäfer, J., Bril, H., Blanc, G., Bossy, A., 2009. Deconvolution of trace element (As, Cr, Mo, Th, U) sources and pathways to surface waters of a gold mining-influenced watershed. Sci. Total Environ. 407, 2063–2076.

Grosbois, C., Courtin-Nomade, A., Robin, E., Bril, H., Tamura, N., Schäfer, J., Blanc, G., 2011. Fate of arsenic-bearing phases during the suspended transport in a gold mining district (Isle river Basin, France). Sci. Total Environ. 409, 4986–4999.

Guo, H., Yang, S., Tang, X., Li, Y., Shen, Z., 2008. Groundwater geochemistry and its implications for arsenic mobilization in shallow aquifers of the Hetao Basin, Inner Mongolia. Sci. Total Environ. 393, 131–144.

Hamberg, R., Bark, G., Maurice, C., Alakangas, L., 2016. Release of arsenic from cyanidation tailings. Miner. Eng. 93, 57–64.

Huang, T., Li, D., 2014. Presentation on mechanisms and applications of chalcopyrite and pyrite bioleaching in biohydrometallurgy-a presentation. Biotechnol. Reports 4, 107–119.

Kaksonen, A.H., Mudunuru, B.M., Hackl, R., 2014. The role of microorganisms in gold processing and recovery-a review. Hydrometallurgy 142, 70–83.

Kim, B.-J., Jang, J.-G., Park, C.-Y., Han, O.-H., Kim, H.-K., 2016. Recycling of arsenic-rich mine tailings in controlled low-strength materials. J. Clean. Prod. 118, 151–161.

Ko, M.-S., Kim, J.-Y., Bang, S., Lee, J.-S., Ko, J.-I., Kim, K.-W., 2012. Stabilization of the As-contaminated soil from the metal mining areas in Korea. Environ. Geochem. Health 34, 143–149.

La Brooy, S.R., Linge, H.G., Walker, G.S., 1994. Review of gold extraction from ores. Miner. Eng. 7, 1213–1241.

Luo, X., Liu, H., Huang, G., Li, Y., Zhao, Y., Li, X., 2016. Remediation of arsenic-contaminated groundwater using media-injected permeable reactive barriers with a modified montmorillonite: sand tank studies. Environ. Sci. Pollut. Res. 23, 870–877.

Manasse, A., Viti, C., 2007. Arsenic adsorption on nanocrystalline goethite: the natural example of bolar earths from Mt Amiata (Central Italy). Environ. Geol. 52, 1365–1374.

Martínez, J., Hidalgo, M.C., Rey, J., Garrido, J., Kohfahl, C., Benavente, J., Rojas, D., 2016. A multidisciplinary characterization of a tailings pond in the Linares-La Carolina mining district, Spain. J. Geochem. Explor. 162, 62–71.

de Mello, J.W.V., Talbott, J.L., Scott, J., Roy, W.R., Stucki, J.W., 2007. Arsenic speciation in arsenic-rich Brazilian soils from gold mining sites under anaerobic incubation. Environ. Sci. Pollut. Res. 14, 388–396.

Ndlovu, S., 2008. Biohydrometallurgy for sustainable development in the African minerals industry. Hydrometallurgy 91, 20–27.

Paktunc, D., Foster, A., Heald, S., Laflamme, G., 2004. Speciation and characterization of arsenic in gold ores and cyanidation tailings using X-ray absorption spectroscopy. Geochim. Cosmochim. Acta 68, 969–983.

Palapa, T.M., Maramis, A.A., 2015. Heavy metals in water of stream near an amalgamation tailing ponds in Talawaan-Tatelu gold mining, North Sulawesi, Indonesia. Procedia Chem. 14, 428–436.

Parviainen, A., Lindsay, M.B.J., Pérez-López, R., Gibson, B.D., Ptacek, C.J., Blowes, D.W., Loukola-Ruskeeniemi, K., 2012. Arsenic attenuation in tailings at a former Cu-W-As mine, SW Finland. Appl. Geochem. 27, 2289–2299.

Ritcey, G.M., 2005. Tailings management in gold plants. Hydrometallurgy 78, 3–20.

Rodríguez-Vila, A., Asensio, V., Forján, R., Covelo, E.F., 2015. Chemical fractionation of Cu, Ni, Pb and Zn in a mine soil amended with compost and biochar and vegetated with *Brassica juncea* L. J. Geochem. Explor. 158, 74–81.

Schippers, A., Nagy, A.A., Kock, D., Melcher, F., Gock, E.-D., 2008. The use of FISH and real-time PCR to monitor the biooxidation and cyanidation for gold and silver recovery from a mine tailings concentrate (Ticapampa, Peru). Hydrometallurgy 94, 77–81.

Soltani, F., Darabi, H., Badri, R., Zamankhan, P., 2014. Improved recovery of a low-grade refractory gold ore using flotation-preoxidation-cyanidation methods. Int. J. Min. Sci. Technol. 24, 537–542.

Tabatabaei, R.H., Nagaraj, D.R., Vianna, S.M.S.M., Napier-Munn, T.J., Gorain, B., 2014. The effect of non-sulphide gangue minerals on the flotation of sulphide minerals from Carlin-type gold ores. Miner. Eng. 60, 26–32.

Tabelin, C.B., Hashimoto, A., Igarashi, T., Yoneda, T., 2014. Leaching of boron, arsenic and selenium from sedimentary rocks: II. pH dependence, speciation and mechanisms of release. Sci. Total Environ. 473-474, 244–253.

Tessier, A., Campbell, P.G.C., Bisson, M., 1979. Sequential extraction procedure for the speciation of particulate trace metals. Anal. Chem. 51, 844–851.

Toujaguez, R., Ono, F.B., Martins, V., Cabrera, P.P., Blanco, A.V., Bundschuh, J., Guilherme, L.R.G., 2013. Arsenic bioaccessibility in gold mine tailings of Delita, Cuba. J. Hazard. Mater. 262, 1004–1013.

Wan, X., Wang, W., Ye, T., Guo, Y., Gao, X., 2006. A study on the chemical and mineralogical characterization of MSWI fly ash using a sequential extraction procedure. J. Hazard. Mater. B 134, 197–201.

Wang, C., Luo, H., Zhang, Z., Wu, Y., Zhang, J., Chen, S., 2014. Removal of As(III) and As(V) from aqueous solutions using nanoscale zero valent iron-reduced graphite oxide modified composites. J. Hazard. Mater. 268, 124–131.

Williams, C., Peng, Y., Dunne, R., 2013. Eucalyptus oils as green collectors in gold flotation. Miner. Eng. 42, 62–67.

Yalcin, E., Kelebek, S., 2011. Flotation kinetics of a pyritic gold ore. Int. J. Miner. Process. 98, 48–54.